A&A 458, 331–337 (2006)
DOI: 10.1051/0004-6361:20065713

Astronomy
&
Astrophysics

Ro-vibrational excitation of the SO molecule by collision with the He atom

F. Lique[1], A. Spielfiedel[1], G. Dhont[2], and N. Feautrier[1]

[1] LERMA and UMR 8112 of CNRS, Observatoire de Paris-Meudon, 92195 Meudon Cedex, France
e-mail: `[francois.lique;annie.spielfiedel]@obspm.fr`
[2] Université du Littoral Côte d'opale, LPCA, 189A avenue Maurice Schumann, 59140 Dunkerque, France

Received 29 May 2006 / Accepted 13 July 2006

ABSTRACT

Context. Over the next few years, ALMA and Herschel missions will perform high spatial and spectral resolution studies at infrared and sub-millimeter wavelengths. This will provide much greater detail about the composition and evolution of molecules in space. Modeling of the spectra will require accurate radiative and collisional rates for species of astrophysical interest.
Aims. We calculate ro-vibrational excitation rate coefficients of SO by He, useful for studies of high-temperature environments.
Methods. A new accurate three dimensional (3D) potential energy surface was calculated for the SO-He system which explicitly takes into account the r-dependence of the SO vibration as well as the R-distance and θ angle which describe the relative position of the collision partners. The dynamics calculations were performed according to the VCC-IOS approximation.
Results. The new rate coefficients between the ro-vibrational levels are calculated for temperatures from 300 K to 800 K.

Key words. ISM: molecules – molecular data – molecular processes

1. Introduction

Observations of molecular emission at millimeter and infrared wavelengths, supplemented by careful and detailed modeling, are powerful tools to investigate the physical and chemical conditions of astrophysical objects. First observed by Gottlieb & Ball (1973) in the interstellar gas, SO has been used extensively to study shocked molecular gas in various environments (Turner et al. 1992; van Dishoeck & Blake 1998; Blake et al. 1987). The modeling of the line intensities requires comparison with model excitation calculations using radiative as well as collisional rates. Collisional excitation in shocked regions and in photon dominated regions involves excitation of high-rotational levels as well as vibrational excitation by the most abundant species, He and H_2.

Rotational excitation rate coefficients for collisions among fine structure levels of SO with He atoms, based on an accurate ab initio potential energy surface (PES), have been calculated recently (Lique et al. 2005; Lique et al. 2006). For pure rotational excitation, the SO r-distance was kept at its equilibrium geometry for the calculation of the PES. In Lique et al. (2005) the sensitivity of the cross sections to different basis sets used in the calculation of the SO-He surface has been studied. In the present paper we focus on calculations of rate coefficients for the $v = 0$–1 vibrational excitation by He. The potential energy surface was calculated for different SO r-distances in order to account for the vibration of SO. The same strategy of calculation of the surface for each SO r-distance as in Lique et al. (2005) was adopted here.

A full close coupling approach for the dynamics calculations is prohibitively expensive in computer time for heavy molecules when transitions among highly excited rovibrational levels are involved. We therefore used the vibrational close-coupling rotational infinite order sudden (VCC-IOS) method (Parker & Pack 1978; Goldflam et al. 1977a,b) to perform the calculations. Cross-sections among the 118 first rotational levels of $v = 0$ and $v = 1$ have been calculated for total energies up to 5000 cm^{-1}. After Boltzmann thermal average, they give rate coefficients up to 800 K.

The paper is organized as follows: Sect. 2 describes the ab initio calculation of the potential energy surface. Section 3 provides a rapid description of the theory and of the calculations. In Sect. 4 we present and discuss our results.

2. Potential energy surface and computation of matrix elements

The present work uses a Jacobi coordinate system, in which r is the SO distance, R is the distance from the center of mass of SO to the He atom and θ is the angle between the two distance vectors ($\theta = 0°$: He adjacent to oxygen atom, $\theta = 180°$: He adjacent to sulfur atom). The SO-He potential energy surface was calculated in the supermolecular approach based on the single and double excitation open-shell coupled cluster method with perturbative contributions of connected triple excitations (RCCSD(T)) computed as defined by Knowles et al. (1993, 2000). To check the validity of this mono-configurational method, we have performed calculations for the first triplet electronic states with the Multi-Configuration Self-Consistent-field (MCSCF) approach. For all investigated geometries, it was found that the weight of the dominant configuration in the ground electronic state of the SO-He complex was between 0.92 and 0.94 which justifies the choice of the RCCSD(T) approach. Calculations were performed for three SO r-distances (2.4, 2.8 and 3.3 bohr) and the same grid of R and θ values (R was assigned values from 4.0 bohr to 16.0 bohr by steps of 0.25 bohr, the angular grid was uniform with a 15 degree spacing from 0 to 180 degree) as described in Lique et al. (2005).The three atoms were described by the

Table 1. Vibrational matrix elements ($\langle v'(r) \mid (r - r_e)^{n-1} \mid v''(r)\rangle$) used in the vibrational averaging of the interaction potential; r_e was taken to be 2.8 bohr.

v'	v''	$n = 1$	$n = 2$	$n = 3$
0	0	1.00000	0.03531	0.00628
0	1	0.00000	0.07084	0.00580
1	1	1.00000	0.05227	0.01790

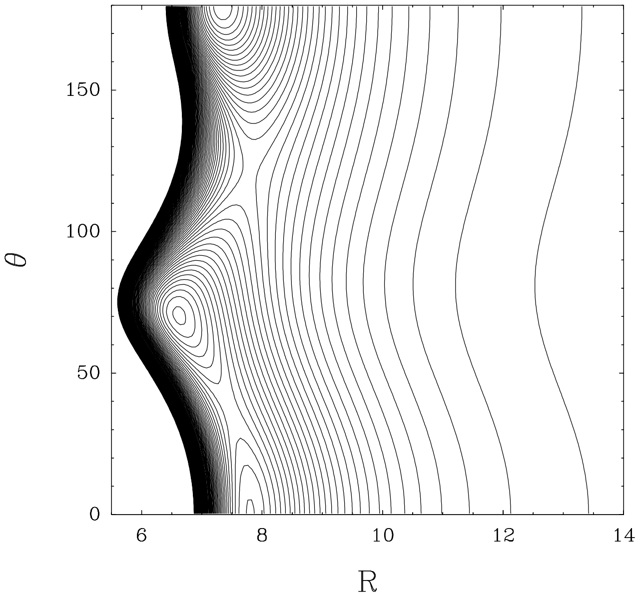

Fig. 1. Contour plot of the $v = 0 \rightarrow v' = 0$ matrix elements of the interaction potential for elastic scattering of He+SO as a function of R and θ. The energies are in cm^{-1} with a distance of 1.0 cm^{-1} between two adjacent contours, the zero of energy is taken as that of the He+SO asymptote.

standard correlation consistent polarized valence quadruple zeta set of Woon & Dunning (1994) augmented by the (3s3p2d2f1g) bond functions optimized by Cybulski & Toczylowski (1999), placed at mid-distance between the SO centre-of-mass and He. In all calculations, the basis set superposition error (BSSE) is corrected at all geometries with the Boys & Bernardi (1970) counterpoise procedure. The PES calculations were performed with the MOLPRO 2002 package (MOLPRO 2002).

The fitting procedure described by Werner et al. (1988) for the CN-He system was adopted in order to obtain the $V(r, R, \theta)$ numerical expansion routine required to perform the dynamical calculations. The potential was fitted to the functional form:

$$V(r, R, \theta) = \sum_{n=1}^{N} \sum_{l=1}^{L_{\max}} d_{m,0}^{l+m-1}(\cos\theta) A_{ln}(R)(r - r_e)^{n-1} \tag{1}$$

where the $d_{m,0}^{l+m-1}(\cos\theta)$ are reduced Wigner rotation matrix elements.

N equals the number of SO bond distances and $L_{\max}$ the number of angles θ for which the potential has been calculated.

For a VCC-IOS calculation, matrix elements of the potential between the vibrational states of the SO molecule are required for fixed values of the Jacobi scattering angle and for all the R-values. We write these matrix elements as:

$$V_{v',v''}(R, \theta) = \langle v'(r) \mid V(r, R, \theta) \mid v''(r)\rangle. \tag{2}$$

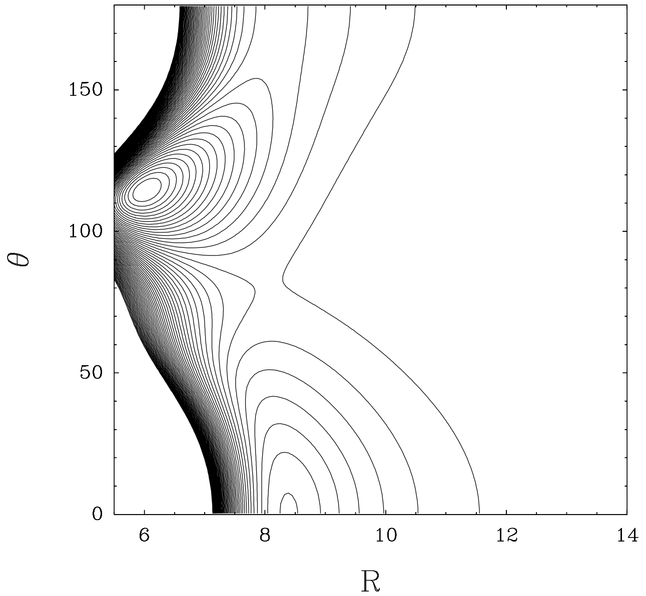

Fig. 2. Contour plot of the $v = 0 \rightarrow v' = 1$ matrix elements of the interaction potential for inelastic scattering of He+SO as a function of R and θ. The energies are in cm^{-1} with a distance of 0.1 cm^{-1} between two adjacent contours, the zero of energy is taken as that of the He+SO asymptote.

The SO vibrational wave functions were obtained by the Fourier grid Hamiltonian (FGH) method of Clay Marston & Balint-Kurti (1989) from a SO potential calculated with the MOLPRO 2002 package at the Complete Active Space Self-Consistent-field (CASSCF) + Multi-Reference Configuration Interaction (MRCI) level using the aug-cc-pVQZ basis set of Woon and Dunning (1994). The vibrational wave functions were taken with $j = 0$. The relevant $\langle v'(r) \mid (r - r_e)^{n-1} \mid v''(r)\rangle$ matrix elements are given in Table 1.

Contour plots of the $V_{0,0}(R, \theta)$ and $V_{0,1}(R, \theta)$ surfaces are respectively shown in Figs. 1 and 2. In these plots the value $\theta = 180°$ corresponds to colinear He-SO. The $V_{1,1}(R, \theta)$ surface is indistinguishable from the $V_{0,0}(R, \theta)$ surface. The global minimum in the $V_{0,0}$ and $V_{1,1}$ surfaces is found to be –34.62 cm^{-1} ($R = 7.35$ bohr, $\theta = 180°$).

3. Calculation of scattering cross sections

In the SO ($^3\Sigma^-$) electronic ground state, the rotational levels are split by spin-rotation coupling. In the intermediate coupling scheme, the rotational wave function of SO can be written for $j \geq 1$ as:

$$\begin{aligned} |F_1 jm\rangle &= \cos\alpha |N = j-1, S\, jm\rangle \\ &\quad + \sin\alpha |N = j+1, S\, jm\rangle \\ |F_2 jm\rangle &= |N = j, S\, jm\rangle \\ |F_3 jm\rangle &= -\sin\alpha |N = j-1, S\, jm\rangle \\ &\quad + \cos\alpha |N = j+1, S\, jm\rangle \end{aligned} \tag{3}$$

where $|N, S\, jm\rangle$ denotes pure Hund's case (b) basis functions and the mixing angle α is obtained by diagonalisation of the molecular Hamiltonian. In the pure case (b) limit, $\alpha \rightarrow 0$, the F_1 level corresponds to $N = j - 1$ and the F_3 level to $N = j + 1$. For SO, the case (b) limit becomes valid beyond $N = 5$. The calculations of the rotational energy levels were done with the F_1, F_2 and F_3

Table 2. Energy in cm^{-1} of the fine structure levels of SO ($v = 0$) ($E = 0$ cm^{-1} for $v = 0, N_J = 1_0$).

Level	N	j	Energy	Level	N	j	Energy	Level	N	j	Energy
1	1	0	0.000	41	14	15	154.021	81	27	26	546.368
2	0	1	1.001	42	14	13	155.147	82	27	27	551.238
3	1	2	3.100	43	14	14	159.835	83	28	29	585.654
4	2	3	6.412	44	15	16	175.565	84	28	27	586.367
5	1	1	10.552	45	15	14	176.641	85	28	28	591.343
6	2	1	10.987	46	15	15	181.358	86	29	30	627.187
7	3	4	11.021	47	16	17	198.538	87	29	28	627.996
8	2	2	13.424	48	16	15	199.571	88	29	29	632.874
9	3	2	14.632	49	16	16	204.314	89	30	31	670.143
10	4	5	16.979	50	17	18	222.941	90	30	29	670.947
11	3	3	17.731	51	17	16	223.938	91	30	30	675.829
12	4	3	19.933	52	17	17	228.701	92	31	32	714.521
13	4	4	23.474	53	18	19	248.774	93	31	30	715.323
14	5	6	24.316	54	18	17	249.739	94	31	31	720.207
15	5	4	26.811	55	18	18	254.521	95	32	33	760.322
16	5	5	30.653	56	19	20	276.036	96	32	31	761.121
17	6	7	33.050	57	19	18	276.974	97	32	32	766.007
18	6	5	35.211	58	19	19	281.772	98	33	34	807.543
19	6	6	39.268	59	20	21	304.727	99	33	32	808.341
20	7	8	43.193	60	20	19	305.642	100	33	33	813.229
21	7	6	45.102	61	20	20	310.454	101	34	35	856.185
22	7	7	49.318	62	21	22	334.847	102	34	33	856.982
23	8	9	54.751	63	21	20	335.742	103	34	34	861.872
24	8	7	56.467	64	21	21	340.566	104	35	36	906.247
25	8	8	60.802	65	22	23	366.396	105	35	34	907.043
26	9	10	67.731	66	22	21	367.272	106	35	35	911.934
27	9	8	69.293	67	22	22	372.107	107	36	37	957.727
28	9	9	73.722	68	23	24	399.372	108	36	35	958.524
29	10	11	82.135	69	23	22	400.234	109	36	36	963.415
30	10	9	83.574	70	23	23	405.078	110	37	37	1010.624
31	10	10	88.077	71	24	25	433.777	111	37	36	1011.422
32	11	12	97.963	72	24	23	434.625	112	37	37	1016.314
33	11	10	99.302	73	24	24	439.477	113	38	39	1064.938
34	11	11	103.865	74	25	26	469.607	114	38	37	1065.738
35	12	13	115.221	75	25	24	470.455	115	38	38	1070.630
36	12	11	116.746	76	25	25	475.303	116	39	40	1120.667
37	12	12	121.088	77	26	27	506.864	117	39	38	1121.470
38	13	14	133.906	78	26	25	507.693	118	39	39	1126.362
39	13	12	135.091	79	26	26	512.557				
40	13	13	139.745	80	27	28	545.547				

functions but, since the dynamical calculations were performed in the IOS approach (the levels are described in the Hund case (b) limit), the usual level labeling N_j with $N = j - 1$, $N = j$, $N = j + 1$ corresponding to the F_1, F_2 and F_3 levels as defined in Eq. (3) will be used in the following.

The energies of the first fine structure levels pertaining to the $v = 0$ and $v = 1$ vibrational levels are given in Tables 2 and 3. They were computed with the experimental spectroscopic constants of Bogey et al. (1982). Due to the low rotational constant there are 118 N_j levels with an energy lower than the first excited vibrational level.

In the VCC-IOS method, the rotational levels are treated as degenerate. Within this approximation the problem reduces to the computation of vibrationally inelastic S-matrix elements calculated with a close coupling approach at fixed θ Jacobi angles for a given L-value. These fixed-angle S-matrix elements must then be mutiplied by the appropriate spherical harmonics and integrated over θ to give the "fundamental IOS cross sections" $\sigma^{\rm IOS}(v, 0 \to v', L)(E)$ out of the $v, N = 0$ level.

In the Hund's case (b) limit, the de-excitation ro-vibrational cross sections are expressed in a reduced form in terms of the $\sigma^{\rm IOS}(v, 0 \to v', L)$ cross sections (Corey & McCourt 1983):

$$\sigma^{\rm IOS}(v, Nj \to v', N'j') = \sum_L (2N+1)(2N'+1)(2j'+1) \begin{pmatrix} N' & N & L \\ 0 & 0 & 0 \end{pmatrix}^2 \times \begin{Bmatrix} L & j & j' \\ S & N' & N \end{Bmatrix}^2 \sigma^{\rm IOS}(v, 0 \to v', L) \tag{4}$$

where ( ) and { } are respectively the "3 – j" and "6 – j" symbols. v, Nj and $v', N'j'$ are the initial and final vibrational and rotational states. The summation in Eq. (4) was performed for $L \leq 79$ which allows us to obtain converged cross sections for rotational angular momenta $N \leq 39$. All the calculations were performed using the MOLSCAT computer program of Hutson & Green (1994). The calculations were carried out using the propagator of Manolopoulos (1986). The reduced mass of the system is 3.694 amu. Typically, the minimum and maximum integration distances are $R_{\rm min} = 3.5\ a_0$ and $R_{\rm max} = 40\ a_0$.

Rate coefficients are obtained by averaging the appropriate cross sections over a Boltzmann distribution of velocities at a

Table 3. Energy in cm^{-1} of the fine structure levels of SO ($v = 1$) ($E = 0$ cm^{-1} for $v = 0, N_J = 1_0$).

Level	N	j	Energy	Level	N	j	Energy	Level	N	j	Energy
1	1	0	1138.020	41	14	15	1290.868	81	27	26	1680.100
2	0	1	1139.019	42	14	13	1292.017	82	27	27	1684.995
3	1	2	1141.110	43	14	14	1296.724	83	28	29	1719.056
4	2	3	1144.405	44	15	16	1312.241	84	28	27	1719.880
5	1	1	1148.634	45	15	14	1313.338	85	28	28	1724.780
6	2	1	1148.984	46	15	15	1318.075	86	29	30	1760.255
7	3	4	1149.060	47	16	17	1335.031	87	29	28	1761.074
8	2	2	1151.483	48	16	15	1336.084	88	29	29	1765.978
9	3	2	1152.666	49	16	16	1340.848	89	30	31	1802.867
10	4	5	1154.900	50	17	18	1359.240	90	30	29	1803.681
11	3	3	1155.756	51	17	16	1360.256	91	30	30	1808.589
12	4	3	1157.916	52	17	17	1365.041	92	31	32	1846.890
13	4	4	1161.454	53	18	19	1384.867	93	31	30	1847.700
14	5	6	1162.182	54	18	17	1385.866	94	31	31	1852.611
15	5	4	1164.733	55	18	18	1390.654	95	32	33	1892.324
16	5	5	1168.575	56	19	20	1411.912	96	32	31	1893.131
17	6	7	1170.850	57	19	18	1412.866	97	32	32	1898.044
18	6	5	1173.060	58	19	19	1417.687	98	33	34	1939.167
19	6	6	1177.121	59	20	21	1440.374	99	33	32	1939.972
20	7	8	1180.915	60	20	19	1441.304	100	33	33	1944.888
21	7	6	1182.867	61	20	20	1446.132	101	34	35	1987.419
22	7	7	1187.090	62	21	22	1470.254	102	34	33	1988.223
23	8	9	1192.384	63	21	20	1471.162	103	34	34	1993.140
24	8	7	1194.138	64	21	21	1476.010	104	35	36	2037.080
25	8	8	1198.483	65	22	23	1501.550	105	35	34	2037.883
26	9	10	1205.262	66	22	21	1502.440	106	35	35	2042.801
27	9	8	1206.859	67	22	22	1507.299	107	36	37	2088.146
28	9	9	1211.300	68	23	24	1534.263	108	36	35	2088.950
29	10	11	1219.552	69	23	22	1535.138	109	36	36	2093.870
30	10	9	1221.023	70	23	23	1540.006	110	37	37	2140.619
31	10	10	1225.539	71	24	25	1568.392	111	37	36	2141.424
32	11	12	1235.256	72	24	23	1569.253	112	37	37	2146.344
33	11	10	1236.623	73	24	24	1574.130	113	38	39	2194.497
34	11	11	1241.202	74	25	26	1603.936	114	38	37	2195.304
35	12	13	1252.377	75	25	24	1604.786	115	38	38	2200.224
36	12	11	1253.658	76	25	25	1609.670	116	39	40	2249.780
37	12	12	1258.287	77	26	27	1640.895	117	39	38	2250.588
38	13	14	1270.914	78	26	25	1641.735	118	39	39	2255.508
39	13	12	1272.123	79	26	26	1646.625				
40	13	13	1276.795	80	27	28	1679.269				

given kinetic temperature T:

$$k_{v,Nj\to v',N'j'} = \left(\frac{8\beta^3}{\pi\mu}\right)^{1/2} \int_0^\infty \sigma(v,Nj \to v',N'j')(E_\mathrm{k}) \times E_\mathrm{k} \exp(-\beta E_\mathrm{k}) dE_\mathrm{k} \quad (5)$$

where $\beta = (k_\mathrm{B}T)^{-1}$, k_B is the Boltzmann constant, μ is the reduced mass of the colliding system. The total energy E is related to the kinetic energy according to $E = E_\mathrm{k} + \epsilon_{v,Nj}$ where $\epsilon_{v,Nj}$ is the energy of the initial rovibrational level. Rate coefficients for the reverse transitions may be obtained by detailed balance.

As the IOS approximation neglects the energy structure of the rotational levels, it is expected to be poor at low energies, so the results presented here refer to high temperatures. The validity of this approach was checked in Lique et al. (2006) for pure rotational excitation. It was found to be appropriate, especially for transitions involving levels with $N > 5$.

However it may not be so applicable to vibrational quenching as resonant vibrational energy transfer may occur. This type of near-resonant energy transfer has been observed experimentally (Stewart et al. 2000; McCaffery & Marsh 2000) and obtained theoretically (Stewart et al. 1988, 2000; Miklavc et al. 1992; Krems et al. 2001) for diatomic molecules with a small moment of inertia (H_2, HF, Li_2). Molecules with smaller rotational constants (CO for example) can exhibit resonant vibrational relaxation when they are initially in very high rotational levels. The role of near-resonant vibrational relaxation has been investigated systematically in CO (Krems 2002). This study shows that the contribution of this resonant process is negligible for low j levels and high energy, and only becomes important when the initial rotational state of $v = 1$ is close in energy to high rotational states of $v = 0$. These cases were not considered in this paper.

4. Results

In order to compute cross sections and rate coefficients for vibrational relaxation of SO, we have tested the convergence of the vibrational close-coupling expansion by including several vibrational wave functions in the basis set.

We first considered the effect of vibrational coupling on the rotational excitation cross sections. Figure 3 compares the fundamental IOS cross sections (see Eq. (4)) for vibrationally elastic

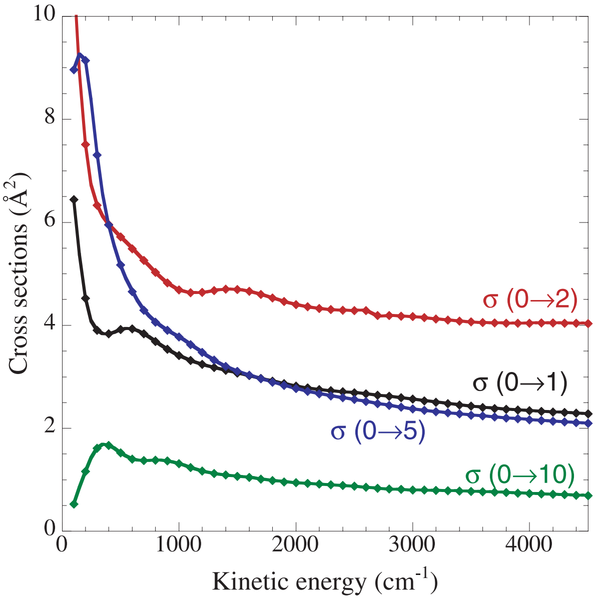

Fig. 3. Variation of the vibrationally elastic rotational cross sections for $v = 0$ with the $v = 0$ and $v = 1$ basis set (full curve) and without vibrational coupling (diamonds).

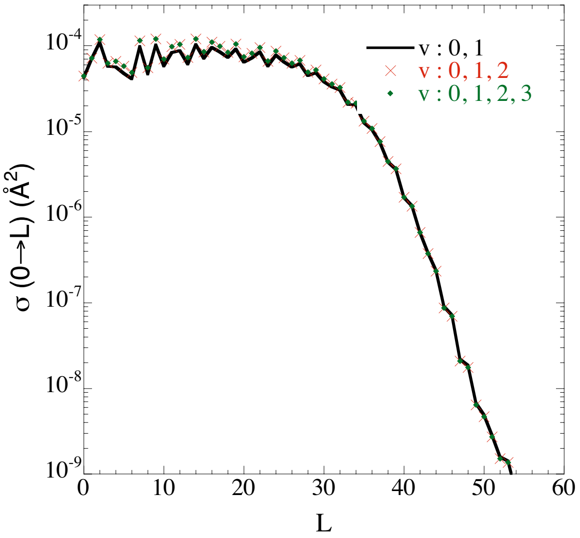

Fig. 4. "Fundamental IOS cross sections" (see Eq. (4)) for vibrationally elastic rotational excitation of SO out of the $v = 1, N = 0$ level to $v = 0, L$ level calculated including 2, 3 and 4 vibrational levels in the dynamical calculations.

rotational excitation of SO out of the $v = 0, N = 0$ level calculated with and without vibrational coupling between $v = 0$ and $v = 1$.

As already found for other systems like CO (Krems 2002) and HF (Krems & Nordholm 2001; Krems et al. 2001), the pure rotational transitions are unaffected by the vibrational channel included in the calculation. This result is directly the consequence of the very small non-diagonal vibrational matrix elements of the interaction potential compared to the diagonal ones. In addition, there is an excellent agreement between the cross sections calculated with the 3D PES and the one previously calculated (Lique et al. 2006) with the 2D PES. This result validates the choice of a 2D PES for pure rotational excitation.

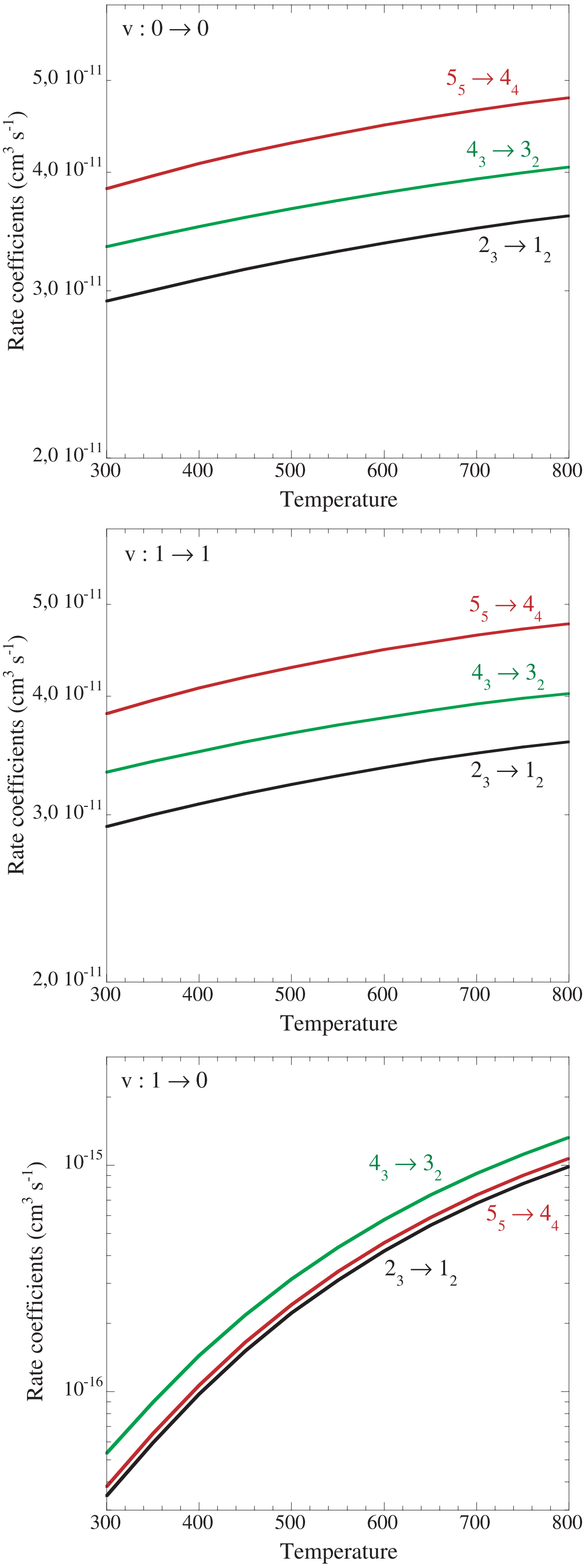

Fig. 5. Temperature variation of the $k_{v,NS\,j\to v',N'S\,j'}$ collision rates for: $v = 0 \to v' = 0$ (*upper panel*), $v = 1 \to v' = 1$ (*medium panel*), $v = 1 \to v' = 0$ (*lower panel*).

We have also considered the convergence of the vibrational expansion on inelastic vibrational cross sections. Figure 4 shows the "fundamental IOS cross sections" out of $v = 1, N = 0$ (see

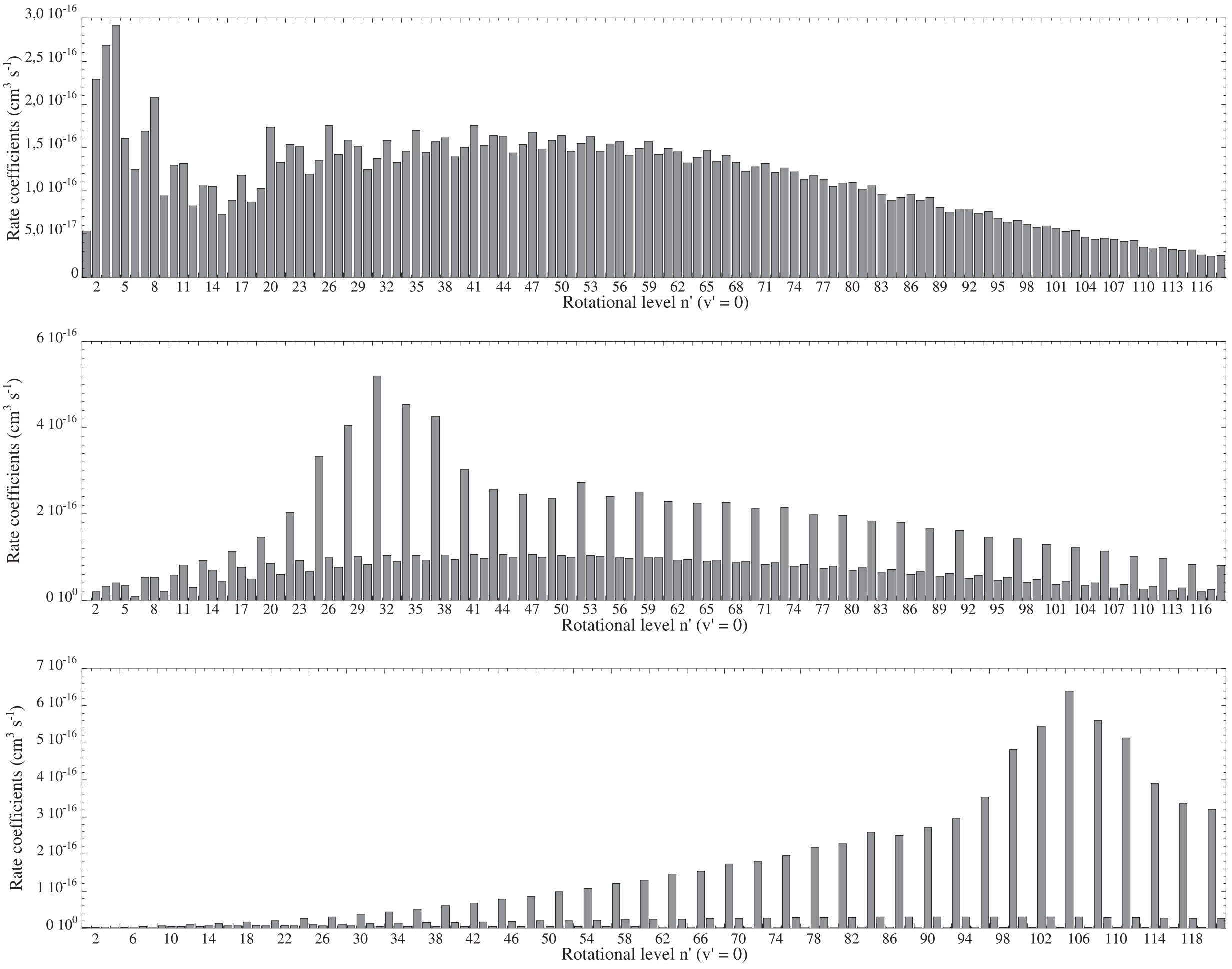

Fig. 6. Distribution of the final fine structure levels $N'_{j'}$ in $v' = 0, n'$ identified by the number n' (given in Table 2 following vibrational relaxation of $v = 1, N_j$ states) at $T = 500$ K. Upper panel is for $N_j = 0_1$ (F_1 level), middle panel is for $N_j = 10_{10}$ (F_2 level) and bottom panel is for $N_j = 35_{34}$ (F_3 level).

Eq. (4)) for vibrational $v = 0, 1$, $v = 0, 1, 2$ and $v = 0, 1, 2, 3$ basis sets.

It follows from this plot that the "fundamental IOS cross sections" from $v = 1$ can be obtained by neglecting coupling with vibrational states higher than $v = 1$. Therefore, all the calculations presented in the following were performed with the $v = 0, 1$ basis set.

Calculations were performed for the 118 first fine structure levels of $v = 0$ and $v = 1$ and for energies up to 5000 cm^{-1} leading to converged rate coefficients for all the considered levels and temperatures up to 800 K. The temperature variation of the rate coefficients involving the first rotational levels are displayed in Fig. 5 for $v = 0 \to v' = 0$, for $v = 1 \to v' = 1$ and for $v = 1 \to v' = 0$ transitions.

One observes a slow variation with temperature of the vibrationally elastic rate coefficients when the variation of the vibrational excitation $v = 0 \to v = 1$ coefficients vary more rapidly. As found for other systems, the rate coefficients for $\Delta v = 1$ transitions are lower than the elastic coefficients by several orders of magnitude. It would be necessary to consider much higher temperatures and/or high-j levels leading to near-resonant j-levels belonging to $v = 0$ and $v = 1$ to get much higher vibrational excitation rate coefficients. It is thus expected that the values obtained in the present VCC-IOS approximation for vibrational excitation and desexcitation give the correct order of magnitude of the rate coefficients.

Figure 6 presents diagrams of the distribution of the final rotational states $v' = 0, N'_{j'}$ (identified by the number n') after vibrational relaxation of various $v = 1, N_j$ states at a temperature of 500 K.

The vibrational relaxation of low j levels exhibits a first peak centered in the region of low j' levels and a second broad peak decreasing slowly for large j' levels. As the initial rotational excitation increases, the first peak becomes larger than the second one and shifts toward larger j' values. One can also observe in this figure a strong propensity for F-conserving transitions in the large j limit. This was already found in pure rotational cross sections and rate coefficients (Lique et al. 2005) and predicted theoretically (Alexander & Dagdigian 1988).

All the rate coefficients are available on our web site (`http://amdpo.obspm.fr/basecol/`).

5. Summary and discussion

In this work, we use the vibrational close coupling - rotational IOS approach to investigate the ro-vibrational energy transfer in collisions of SO with He atoms. The calculations are performed with a new accurate 3D potential energy surface. The results can be summarized as follows:

(i) The vibrationally elastic rotational energy transfer in $v = 0$ is essentially unaffected by the vibrational coupling with $v = 1$.

An analogous behaviour has been observed by Krems & Nordholm (2001) in their study of vibrational and rotational excitation of HF by collisions with Ar. From an analysis of the rotational excitation of HF ($v, j = 0$) for different v-values, these authors conclude that the vibrational motion of HF plays no role in pure rotational transitions. This result, if confirmed for other colliding systems, is important as cross sections and rate coefficients for rotational excitation may be obtained without considering the vibration of the diatomic molecule.

(ii) In the energy range considered ($T \leq 800$ K) the rate coefficients for vibrational excitation of $v = 1$ are several orders of magnitude lower than the rotational rate coefficients. As a consequence, vibrational excitation of SO by He may be considered as negligible in comparison with radiative vibrational excitation in the majority of non-Local Thermodynamic Equilibrium (LTE) astrophysical environments.

(iii) The calculations performed within the VCC-IOS approximation cannot take into account the near-resonant interactions that may occur between highly excited rotational levels in $v = 0$ and $v = 1$. Such an effect is small for low or moderately high rotational levels and high energies.

It is difficult to assess the absolute accuracy of our calculated rates. The typical error may be lower than an order of magnitude, and we believe that the results are probably accurate within a factor of 2–3. Some caution must be exercised concerning the use of the present rate coefficients for collisions with He to provide a first estimate of rate coefficients with para-H_2 ($j = 0$). The underlying approximation is to consider identical cross sections for the two colliding systems and apply a scaling factor to account for the different associated reduced masses. Recent results on rotational excitation of CO (Wernli et al. 2006), SiO (Dayou & Balança 2006) and CS (Lique 2006) pointed out that rate coefficients with para-H_2 ($j = 0$) are within a factor 1–3 larger or lower than those with He, depending on the selected transition. This indicates that accurate rate coefficients for collisions with H_2 cannot be obtained from the present results although they give the correct order of magnitude.

Acknowledgements. The calculations of ab initio potential energy surfaces were performed on the parallel machine MPOPM of Paris Observatory, and the scattering calculations were performed at the IDRIS-CNRS center (Institut de Développement et des Ressources en Informatique Scientifique du Centre National de la Recherche Scientifique) under project 050883.

References

Alexander, M. A., & Dagdigian, P. J. 1988, J. Chem. Phys., 79, 302
Blake, G. A., Surron, E. C., Masson, C. R., & Phillips, T. G. 1987, ApJ, 315, 621
Basecol: `http://amdpo.obspm.fr/basecol/`
Bogey, M., Demuynck C., & Destombes, J. L. 1982, Chem. Phys., 66, 99
Boys, S. F., & Bernardi, F. 1970, Mol. Phys., 19, 553
Clay Marston, C., & Balint-Kurti, G. G. 1989, J. Chem. Phys., 91 3571
Corey, G., & McCourt, F. R. 1983, J. Chem. Phys., 87, 2723
Cybulski, S. M., & Toczylowski, R. R. 1999, J. Chem. Phys., 111, 10520
Dayou, F., Balança, C. 2006, A&A, submitted
Goldflam, R., Green, S., & Kouri, D. J. 1977a, J. Chem. Phys., 67, 4149
Goldflam, R., Kouri, D. J., & Green, S. 1977b, J. Chem. Phys., 67, 5661
Gottlieb, C. A., & Ball, J. A. 1973, ApJ, 184, L59
Hutson, J. M., & Green, S. 1994, MOLSCAT computer code, version 14, Collaborative Computational Project No. 6 of the Science and Engineering Research Council, UK
Knowles, P. J., Hampel, C., & Werner, H.-J. 1993, J. Chem. Phys., 99, 5219
Knowles, P. J., Hampel, C., & Werner, H.-J. 2000, J. Chem. Phys., 112, 3106
Krems, R. V. 2002, J. Chem. Phys., 116, 4517
Krems, R. V., & Nordholm, S. 2001, J. Chem. Phys., 115, 257
Krems, R. V., Markovic, N., Buchachenko, A. A., & Nordholm, S. 2001, J. Chem. Phys., 114, 1249
Lique, F. 2006, unpublished data
Lique, F. Spielfiedel, S., Dubernet M.-L., & Feautrier, N. 2005, J. Chem. Phys., 123, 134316
Lique, F. Spielfiedel, S. & Feautrier, N. 2006, A&A, 450, 399
McCaffery, A. J., & Marsh, R. J. 2000, J. Phys. Chem., 104, 10442
Manolopoulos, D. E. 1986, J. Chem. Phys., 85, 6425
Miklavc, A., Markovic, N., Nyman., G., Harb., V., & Nordholm., S. 1992, J. Chem. Phys., 97, 3348
MOLPRO is a package of ab initio programs written by: Werner, H.-J., & Knowles, P. J. with contributions from Almlöf, J., Amos, R. D., Deegan, M. J., et al.
Parker, G. A., & Pack, R. T. 1978, J. Chem. Phys., 68, 1585
Stewart, B., Magil, P. D., Scott, T. P., Derouard, J., & Pritchard, D. E. 1988, Phys. Rev. Lett., 60, 282
Stewart, B., Magil, P. D., & Pritchard, D. E. 2000, J. Phys. Chem., 104, 10565
Turner, B. E., Chan, K.-W., Green, S., & Lubowich, D. A. 1992, ApJ, 399, 114
van Dishoeck, E. F., & Blake G. A., 1998, ARA&A, 36, 317
Wernli, M., Valiron, P., Faure, A., et al. 2006, A&A, 446, 367
Werner, H.-J., Follmeg B., Alexander, M. H., & Lemoine D. 1988, J. Chem. Phys., 89, 3139
Woon, D. E., & Dunning, T. H. Jr 1994, J. Chem. Phys., 100, 2975